



HAL
open science

Fatigue Life Predictions for a European Pavement Test Section Subjected to Individual and Platoon Truck Configurations

Paulina Leiva-Padilla, Juliette Blanc, Aitor Salgado, Ferhat Hammoum,
Pierre Hornyh

► **To cite this version:**

Paulina Leiva-Padilla, Juliette Blanc, Aitor Salgado, Ferhat Hammoum, Pierre Hornyh. Fatigue Life Predictions for a European Pavement Test Section Subjected to Individual and Platoon Truck Configurations. *Transportation Research Record*, 2022, 2676 (4), pp. 746-762. 10.1177/03611981211065430 . hal-03658248

HAL Id: hal-03658248

<https://hal.science/hal-03658248>

Submitted on 3 May 2022

HAL is a multi-disciplinary open access archive for the deposit and dissemination of scientific research documents, whether they are published or not. The documents may come from teaching and research institutions in France or abroad, or from public or private research centers.

L'archive ouverte pluridisciplinaire **HAL**, est destinée au dépôt et à la diffusion de documents scientifiques de niveau recherche, publiés ou non, émanant des établissements d'enseignement et de recherche français ou étrangers, des laboratoires publics ou privés.

1 **Fatigue life predictions for a European pavement test section**
2 **subjected to individual and platoon truck configurations**

3
4 **Paulina Leiva-Padilla (corresponding author)**

5 Materials and Structures Department (MAST-MIT)

6 French Institute of Science and Technology for Transport, Development and Networks (IFSTTAR)

7 Gustave Eiffel University, Campus Nantes

8 F-44344 Bouguenais, France

9 ORCID number: <https://orcid.org/0000-0002-3650-859X>

10 E-mail: paulina.leiva-padilla@univ-eiffel.fr

11
12 **Juliette Blanc**

13 Materials and Structures Department (MAST-LAMES)

14 French Institute of Science and Technology for Transport, Development and Networks (IFSTTAR)

15 Gustave Eiffel University, Campus Nantes

16 F-44344 Bouguenais, France

17 ORCID number: <https://orcid.org/0000-0002-3462-2436>

18 E-mail: juliette.blanc@univ-eiffel.fr

19
20 **Aitor Salgado**

21 Applus IDIADA Group

22 L'Albornar 43710 Santa Oliva, Tarragona, Spain

23 E-mail: aitor.salgado@idiada.com

24
25 **Ferhat Hammoum**

26 Materials and Structures Department (MAST-MIT)

27 French Institute of Science and Technology for Transport, Development and Networks (IFSTTAR)

28 Gustave Eiffel University, Campus Nantes

29 F-44344 Bouguenais, France

30 ORCID number: <https://orcid.org/0000-0001-8449-9707>

31 E-mail: ferhat.hammoum@univ-eiffel.fr

32
33 **Pierre Hornych**

34 Materials and Structures Department (MAST-LAMES)

35 French Institute of Science and Technology for Transport, Development and Networks (IFSTTAR)

36 Gustave Eiffel University, Campus Nantes

37 F-44344 Bouguenais, France

38 ORCID number: <https://orcid.org/0000-0002-8733-9095>

39 E-mail: pierre.hornych@univ-eiffel.fr

40
41 Word Count: 238 words abstract + 5029 words text + 30 words acknowledgements + 868 words
42 references + 951 words tables = 7116 (limit 7500)

43
44 Submission Date: August 1, 2021

Published in Transportation Research Record, Vol 2676, Issue 4, 2022. Sage Publications Inc

<https://doi.org/10.1177/03611981211065430>

1 **ABSTRACT**

2
3 Truck platooning for the transportation of loads is a strategy recently proposed by the automotive
4 sector to cope with traffic congestion, fuel consumption, and operational costs. This new form to
5 configure trucks changes the typical solicitations the pavements structures are used to experience.
6 In this sense, the research efforts of the pavement sector should be aligned with the automotive
7 sector to propose road-friendly platoon configurations. This is one of the objectives of the European
8 project ENSEMBLE. ENSEMBLE, as indicated by its acronym, works on Enabling Safe Multi-
9 Brand pLatooning for Europe. In this context, the present study presents a real scale test done in
10 the Applus IDIADA facilities to evaluate the fatigue behavior of a pavement structure subjected to
11 individual and platoon truck configurations. The effects of parameters as traffic distribution along
12 the year and along the time of the day, percentage of platoons, truck loads, number of trucks in
13 platoon configuration, lateral wandering, and inter-truck distances were evaluated. The study's
14 findings revealed that the reduced rest times between trucks in the platoon configuration reduce
15 the recovery time of the asphalt layers, increasing the fatigue damage of the pavement at high
16 temperature conditions. This underlines the need for further research to allow the proper
17 implementation of truck platoons. For example, research is needed to define strategies to make
18 truck platoon configurations more pavement-friendly and analyze the costs associated with the
19 changes in the required road maintenance/rehabilitation treatments, among others.

20
21 **Keywords:** individual truck, platoon, fatigue life, pavement.
22

1. INTRODUCTION

Partially or fully self-driven trucks in platoon configurations are part of the most recent and innovative advances presented by automotive companies in the last decade [1]–[3]. These technologies seem to be capable of providing benefits in terms of reducing congestion for a better traffic flow, improving the braking/acceleration abilities of the vehicles, reducing fuel consumption, and more generally reducing operating costs of the vehicles and enhancing road safety [1], [2], [4]–[17].

However, platooning trucks introduce new traffic multi-load configurations with the following two characteristics: (1) reduced deviation of the lateral position of the vehicles forming the platoon and therefore load channelization [1], [4], [17]–[24] and (2) reduced inter-truck distances between the trucks in the platoon, which may hinder the self-healing capacity of asphalt concrete materials [4], [17], [22]. In this sense, a truck platoon deployment without precaution could accelerate pavement damage in terms of lower fatigue cracking/permanent deformation life [1], [4], [17], [20], [21], [23], [24] and lead to earlier rehabilitation/maintenance treatments [18], [23].

In this context, since 2018, the European Union has been developing a research project called ENSEMBLE. ENSEMBLE’s objectives are to pave the way for adopting multi-brand truck platooning in Europe to improve fuel economy, traffic safety, and throughput [2], [3].

ENSEMBLE is a European project co-funded under the Horizon2020 Research and Innovation Programme, grant agreement No 769115. This project is coordinated by the TNO (The Netherlands Organization), and associates main European trucks manufacturers (DAF, DAIMLER Truck, IVECO, MAN, SCANIA, VOLVO Group), the European Association of Automotive Suppliers (CLEPA), ERTICO (European Road Transport Telematics Implementation Coordination Organization, which is a link with the European Truck Platooning Community), and several research organizations: IDIADA, Gustave Eiffel University, KTH, and VU Brussel.

ENSEMBLE is composed of five work packages that integrate the different sectors related to the truck platoon development tasks in Europe. WP1 is related to Management, WP2 to Specification of a generic solution, WP3 to Platooning In-Vehicle Technology, and WP4, from which is part of this document, to Infrastructure, Logistics, and Impact analysis.

In this regard, the objective of this paper was to assess the effect that individual and platoon truck configurations can produce on the fatigue service life of a real scale pavement section located in the test track facilities of Applus IDIADA in Tarragona, Spain, which are commonly used for vehicle testing and development activities. The approach used in this project is based on an original fatigue model, developed by Homsí et al. [25]–[27] to consider the effects of multiple axle loads. This model was used to evaluate the fatigue life of the pavement structure for three potential scenarios of truck platooning, using a mechanistic-empirical approach based on the cumulative damage concept.

1.1. Cumulative damage

Miner's rule is the most popular and widely used damage model for materials [28]. As shown in Equation 1, Miner's rule states that damage (D) can be predicted by the linear accumulation of fatigue damage fractions due to each individual cycle, until failure occurs.

$$D = \sum_{i=1}^T \frac{n_i}{N_{fi}} \geq 1 \quad (1)$$

With n_i : the number of cycles at each stress amplitude level, N_{fi} : the number of cycles to failure for the stress amplitude of interest, and T : total number of load sequences.

For asphalt materials, different test protocols are used to define fatigue equations to determine the number of cycles to failure according to different strain/stress levels. In Europe, several test protocols are standardized by the European Committee for Standardization (CEN) under the EN 12697-24. New protocols have been recently defined to try to extend these fatigue equations to more complex loading conditions (non-sinusoidal signals, multiple loads). In the model proposed by Homsy et al. [18], new parameters are introduced, based on the shape of the strain signal obtained by the passage of multi-axle configurations.

1.2. Fatigue test protocols for asphalt materials in Europe

Based on EN 12697-24, there are six fatigue tests used in Europe to study the fatigue behavior of asphalt materials. Table 1 summarizes the test conditions applied in these six tests, as well as the fatigue equation proposed to fit the results. The different fatigue models are expressed by relationships between the applied cyclic strain or stress and the logarithm of the number of cycles to failure when specific temperature and frequency conditions are applied.

TABLE 1 Some standard protocols of testing in Europe according to EN 12697-24 [29].

Fatigue Test	Fatigue equation	Variables	Test conditions
Two points bending fatigue test on trapezoidal shaped specimen.	$\log(N) = a + \left(\frac{1}{b}\right) \log(\varepsilon)$	N : loading cycles. ε : relative maximum strain. a : intercept obtained by regression. $\frac{1}{b}$: fatigue curve slope.	<u>Load mode of testing</u> : displacement (3 strain levels). <u>Frequency</u> : 25 ± 1 Hz, sinusoidal in the upper part of the specimen with an amplitude = $\pm 5 \mu\text{m}$. <u>Temperature</u> : $10 \pm 1^\circ\text{C}$. <u>Failure criteria</u> : conventional (stiffness = 50% of initial value).
Two points bending fatigue test on prismatic shaped specimen.	$\ln(N_{ij}) = A_0 + A_1 \ln(\sigma_{jmax})$	N_{ij} : fatigue life specimen i for the tension level σ_{jmax} . A_0 : intercept obtained by regression. A_1 : fatigue curve slope. σ_{jmax} : maximum relative tension.	<u>Load mode of testing</u> : load (3 tension levels). <u>Frequency</u> : 25 ± 1 Hz, sinusoidal in the upper part of the specimen. <u>Temperature</u> : not specified, can be -20 to $30 \pm 1^\circ\text{C}$. <u>Failure criteria</u> : once reached a displacement = $280 \mu\text{m}$.
Three points bending fatigue test on prismatic shaped specimen.	$\varepsilon = k_1 * N^{k_2}$	ε : instantaneous strain or half of the cyclic amplitude for the strain function at cycle 100. k_1, k_2 : fatigue law coefficients obtained by regression. N : total number of cycles.	<u>Load mode of testing</u> : displacement (3 displacement levels). <u>Frequency</u> : 10 Hz, sinusoidal with a total amplitude $2D_0 = 80 \mu\text{m}$ to $350 \mu\text{m}$. <u>Temperature</u> : $20 \pm 1^\circ\text{C}$. <u>Failure criteria</u> : amplitude for cycle N is equal to half the amplitude of the cyclic load calculated for cycle 100, $(1/2 \varepsilon_c(100))$.

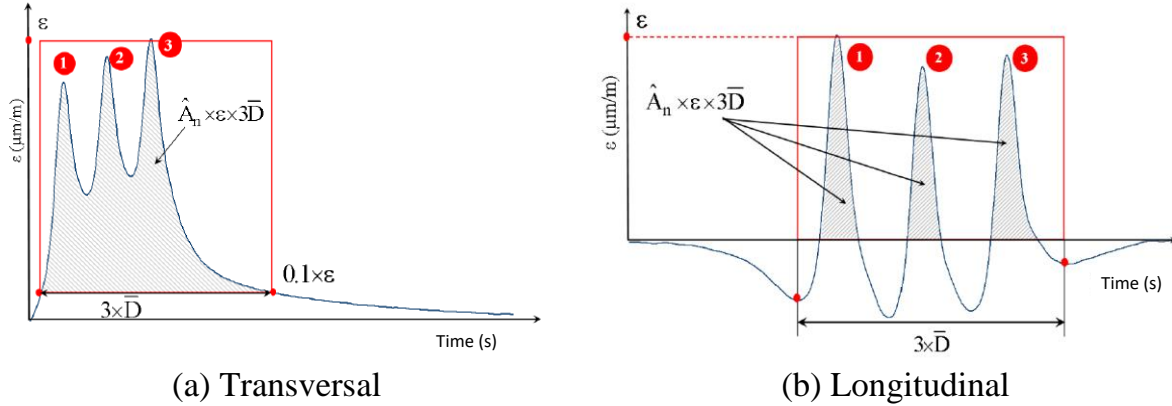
Four-point bending test on prismatic shaped specimens.	$\ln(N_{i,j,k}) = A_0 + A_1 * \ln(\varepsilon_i)$	N : fatigue life. i : specimen number. j : failure criteria selected. k : test conditions. ε_i : initial strain amplitude, measured at 100 cycle.	<u>Load mode of testing</u> : constant load or displacement (3 levels). <u>Frequency</u> : 0,1 to 60 Hz±0,1 Hz, sinusoidal. <u>Temperature</u> : 0 and 20±1°C. <u>Failure criteria</u> : conventional (stiffness = 50% of initial value)., but can be changed, should be indicated.
Indirect Tensile Test on cylindrical specimens.	$\log(N_f) = \log(k_\varepsilon) + n_\varepsilon * \log(\varepsilon_0)$ <u>Energy coefficient approach</u> : $\log(N_{f,w}) = \log(k_w) + n_w * \log(\varepsilon_0)$	N_f : loading cycles. $k_\varepsilon, n_\varepsilon$: regression parameters obtained from fatigue curve. N_f : loading cycles to fatigue for the resilience method. $k_\varepsilon, n_\varepsilon$: regression parameters obtained from fatigue curve for the resilience method.	<u>Load mode of testing</u> : constant load for the generation of a constant diametral stress tension. <u>Frequency</u> : 10Hz, indirect traction stress controlled, initial strain level in a range of 70 µm/m and 400 µm/m, 3 stress levels, load type haversine with loading time = 0.1 s and rest period = 0.4 s, <u>Temperature</u> : -10 to 30±0,5°C (10°C standard temperature). <u>Failure criteria</u> : cycles to fracture, but can be changed, should be indicated.
<u>Fatigue test</u> : Cyclic Indirect Tensile Test on cylindrical shaped specimens.	$\log(N_f) = \log(k_\varepsilon) + n_\varepsilon * \log(\varepsilon_0)$ <u>Energy coefficient approach</u> : $\log(N_{f,w}) = \log(k_w) + n_w * \log(\varepsilon_0)$	N_f : loading cycles. $k_\varepsilon, n_\varepsilon$: regression parameters obtained from fatigue curve. N_f : loading cycles to fatigue for the resilience method. $k_\varepsilon, n_\varepsilon$: regression parameters obtained from fatigue curve for the resilience method.	<u>Load mode of testing</u> : compression cyclic load for the generation of a uniform diametral stress tension. <u>Frequency</u> : 10Hz, sinusoidal without rest periods. <u>Temperature</u> : 20±0,5°C. <u>Failure criteria</u> : energy coefficient based in the dissipated energy approach.

1
2 Considering that the equations described in Table 1 do not consider the effect produced by multiple
3 axle configurations, Homsí et al. [25]–[27], [30] proposed the fatigue model shown in Equation 2.
4 Homsí’s model is based on the laboratory reproduction of 12 synthetic strain signals obtained from
5 the real strain signals obtained from the Accelerated Pavement Testing facility of IFSTTAR-
6 Gustave Eiffel University (from the French acronym: French Institute of Science and Technology
7 for Transport, Development, and Networks) under single, tandem and tridem axles. The laboratory
8 test used to reproduce the 12 synthetic signals was the 2-point bending fatigue test, on trapezoidal
9 specimens conditioned at 20°C (common European fatigue test standardized as UNE EN 12697-
10 24 [22]), which was adapted to apply frequencies ranging from 8.33 Hz to 40 Hz and strain levels
11 ranging from 47 µm/m to 550 µm/m. The fatigue failure criterion used to calibrate the model
12 considers the point when there is a 50% reduction in the initial stiffness value of the material.
13

$$\log(N_f) = a \log(\varepsilon) + b * \log(Np) + c * \hat{A}n + d * \bar{D} + e \quad (2)$$

[25]–[27], [30]

14 Where (see Figure 1), ε : strain intensity (peak strain level) produced by the passage of the reference
15 axle (tridem axle in the example of Figure 1), Np : number of peaks of the strain signal (1 for single
16 axles, 2 for double axles and 3 for tridem axles), $\hat{A}n$: positive area under the loading signal in the
17 transversal/longitudinal direction divided by the peak strain and its duration, and \bar{D} : Duration of
18 the loading signal divided by the number of peaks (in seconds).



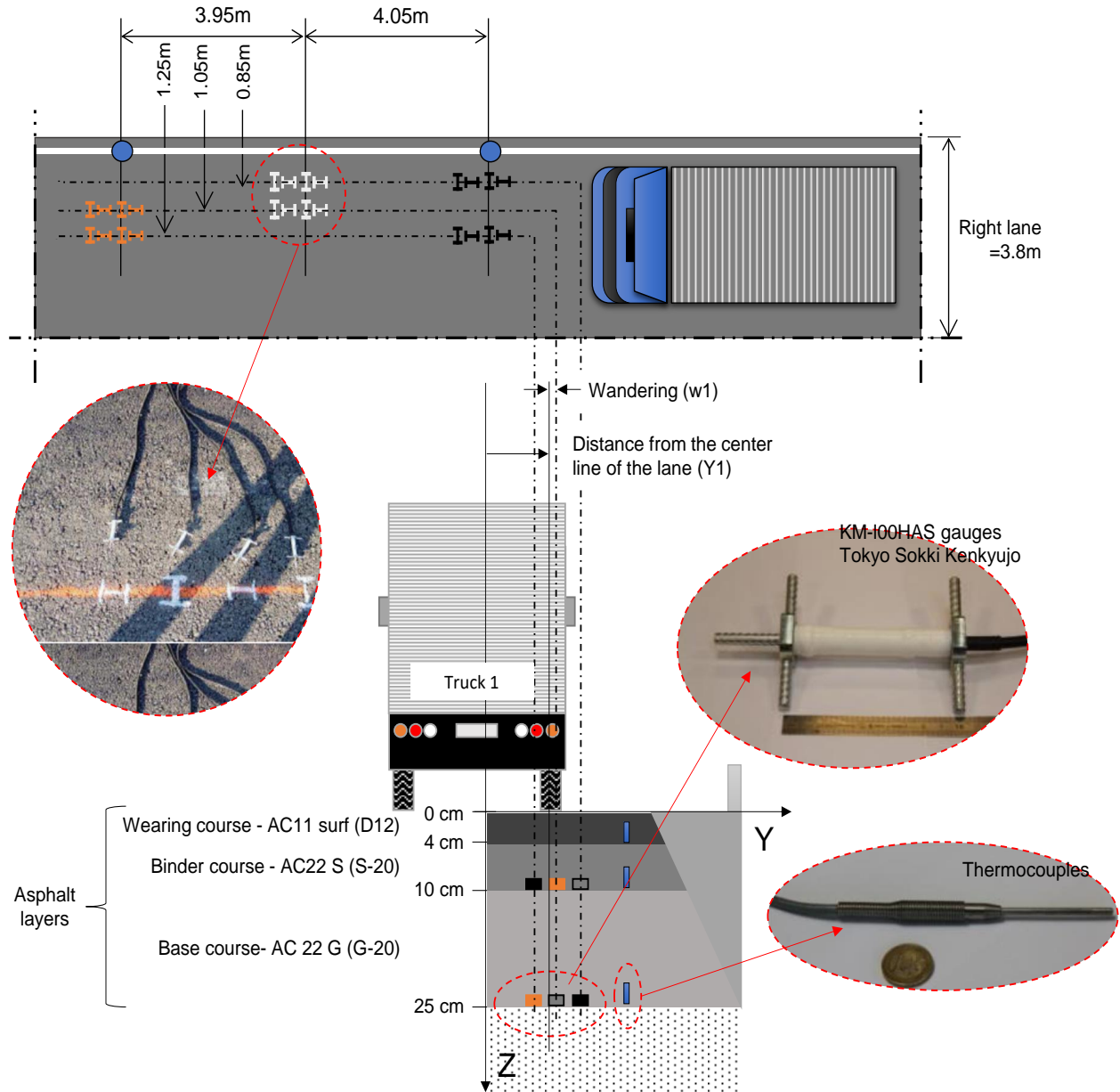
1 (a) Transversal
 2 (b) Longitudinal
 3 **FIGURE 1 Example of parameters used to characterize the transversal/longitudinal strain**
 4 **signals of a tridem axle (reprinted from [25]).**

5 **2. FULL SCALE EXPERIMENT**

6 **2.1. Pavement section and instrumentation**

7
 8 The test section used in the study was located in the facilities of the automotive company IDIADA,
 9 in Tarragona, Spain. The pavement structure consisted of 3 asphalt layers: a 4 cm thick wearing
 10 course, a 6 cm thick binder course, and a 15 cm thick base course. According to the standard UNE
 11 EN 13108-1, the types of asphalt mixture for each layer are respectively: asphalt concrete mixture
 12 with 11 mm maximum particle size used for surface layers (AC11 surf (D12)), semi-dense graded
 13 asphalt concrete mixture with 20 mm maximum particle size (AC 22 S (S-20)), and coarse graded
 14 asphalt concrete mixture with 22 mm maximum particle size (AC 22 G (G-20)). The mixtures were
 15 manufactured with a polymer-modified binder type PMB 45-80/65 according to the UNE-EN
 16 14023, reaching densities of 2.38 to 2.39 g/cm³ and air voids of 4.7% to 6.8%.

17
 18 As shown in Figure 2, the section was instrumented with an array of 24 strain gauges type KM-
 19 100HAS Tokyo Sokki Kenkyujo, placed at 0.85m, 1.05m, and 1.25 from the edge of the right lane.
 20 12 strain gauges (6 longitudinal and 6 transversal), were placed at the bottom of the binder course
 21 and 12 other gauges at the bottom of the base course. Thermocouples were also installed at the
 22 bottom of each asphalt layer, to measure the temperature conditions during the tests.



1
2 **FIGURE 2 Schema of the pavement structure and instrumentation (not to scale).**

3 **2.2. Test protocol**

4
5 The objective of the tests was to compare the pavement response under individual trucks and trucks
6 in platoon configuration. Two test campaigns were performed, one in the winter, and one in the
7 summer, to cover both cold and hot temperature conditions. The different test conditions are
8 summarized in Table 2 and Figure 3, and include:

- 9 i. two test campaigns, one done in the winter and the other in the summer,
10 ii. 20 cm of lateral deviation (wandering) for the first four strain signals and addition of 4
11 extra strain signals with a lateral deviation (wandering) increased to 40 cm during the
12 summer campaign (see Figure 3b),
13 iii. lateral offset of 0 cm from the centerline of the lane (see Figure 3b),

- 1 iv. inter-truck distances adjusted to a time gap of 0.8s,
- 2 v. four truck speed values,
- 3 vi. individual and platoon truck load configurations.
- 4

TABLE 2 Parameters evaluated in the experimental program.

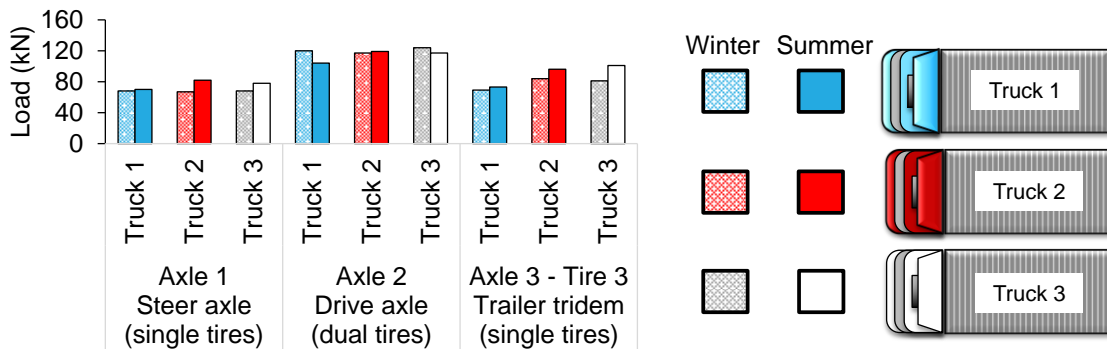
Parameter	Characteristics
Pavement responses: horizontal strains	Depth of measurement: <ul style="list-style-type: none"> • 10 cm (4cm of a wearing course + 6cm of a binder course). • 25 cm (4cm of a wearing course + 6cm of a binder course + 15 cm of a base course). Direction of measurement: <ul style="list-style-type: none"> • Longitudinal. • Transversal.
Lateral deviation (wandering)	20 cm: 4 strain signals for winter/summer and individual/platoon, at each test speed. 40 cm: additional 4 strain signals (8 strain signals in total) for platoon and summer at each test speed. Lateral deviation (wandering) between platoons and between trucks. Values measured with the laser system shown in Figure 4.
Lateral offset	0 cm from the center line of the lane.
Inter-truck distance	Adjusted to a time gap of 0.8 s between trucks. Values measured with the laser system shown in Figure 4.
Campaigns and truck configurations	Winter: <ul style="list-style-type: none"> • 11 of January 2020: <ul style="list-style-type: none"> ○ Configuration: Individual trucks ○ Temperature: 10.3°C and 11.3°C respectively at 25cm and 10cm depth from the pavement surface. • 12 of January 2020: <ul style="list-style-type: none"> ○ Configuration: Platoon. ○ Temperature: 8.3°C and 6.1°C respectively at 25cm and 10cm depth from the pavement surface. Summer: <ul style="list-style-type: none"> • 29 of August 2020: <ul style="list-style-type: none"> ○ Configuration: Individual trucks ○ Temperature: 27.5°C and 25.9°C respectively at 25cm and 10cm depth from the pavement surface. • 30 of August 2020: <ul style="list-style-type: none"> ○ Configuration: Platoon. ○ Temperature: 25.7°C and 25.0°C respectively at 25cm and 10cm depth from the pavement surface.
Truck load	≈48 ton, fully loaded semitrailer truck limits defined by the EU (see details per axle type in Figure 3a).
Truck speed	40, 60, 70 and 80 km/h (EU speed limits defined for heavy trucks circulation). Values measured with the laser system shown in Figure 3c.
Number of passages	Winter: <ul style="list-style-type: none"> • Individual configuration: 4 speeds x 2 repetitions x 3 trucks = 24 passages. • Platoon configuration: 4 speeds x 5 repetitions = 20 passages. • Total passages = 44. Summer: <ul style="list-style-type: none"> • Individual configuration: 4 speeds x 2 repetitions x 3 trucks = 24 passages. • Platoon configuration: 4 speeds x 5 repetitions = 20 passages. • Total passages = 44

6

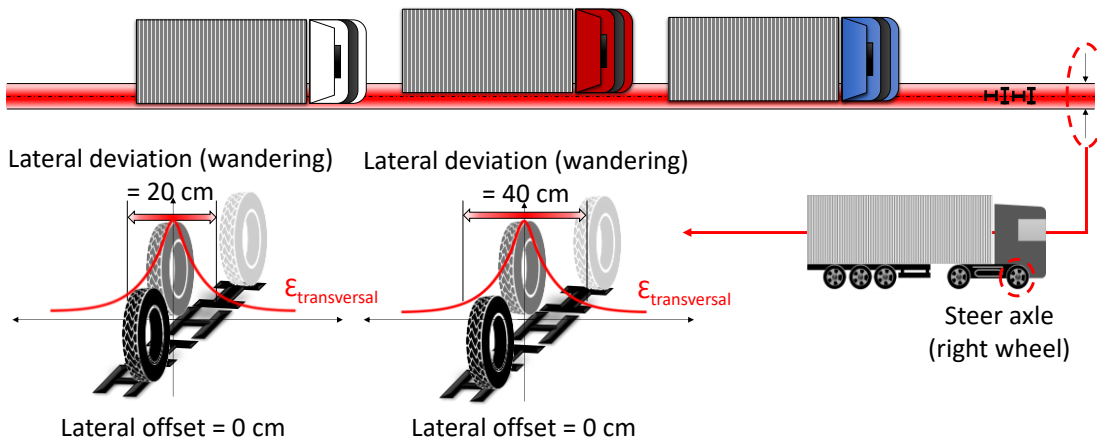
1 Three 5-axle human-driven semi-trailer trucks, fully loaded at their maximum legal load in Europe
 2 (40 tons), were used for each test campaign. The main characteristics of the vehicles used are shown
 3 in Figure 3a. The use of human-driven trucks following platoon truck configurations is the cause
 4 of the variation in the loads per truck and test campaign. Figure 4 shows the laser system used to
 5 measure the ability of the human drivers to follow platoon truck configurations. The parameters
 6 measured by the laser system were the truck speed, lateral deviation (wandering), and inter-truck
 7 distances.

8
 9 The tests were performed first with each individual truck and then with the platoon configuration
 10 for each test condition. The longitudinal/transversal strains were measured at the bottom of the
 11 binder course and base course during each truck passage. Four strain signals per truck speed were
 12 selected to analyze the fatigue behavior in the first lateral wandering interval. And four additional
 13 strain signals were added to the analysis of the summer campaign to study the effect of increasing
 14 the wandering.

15

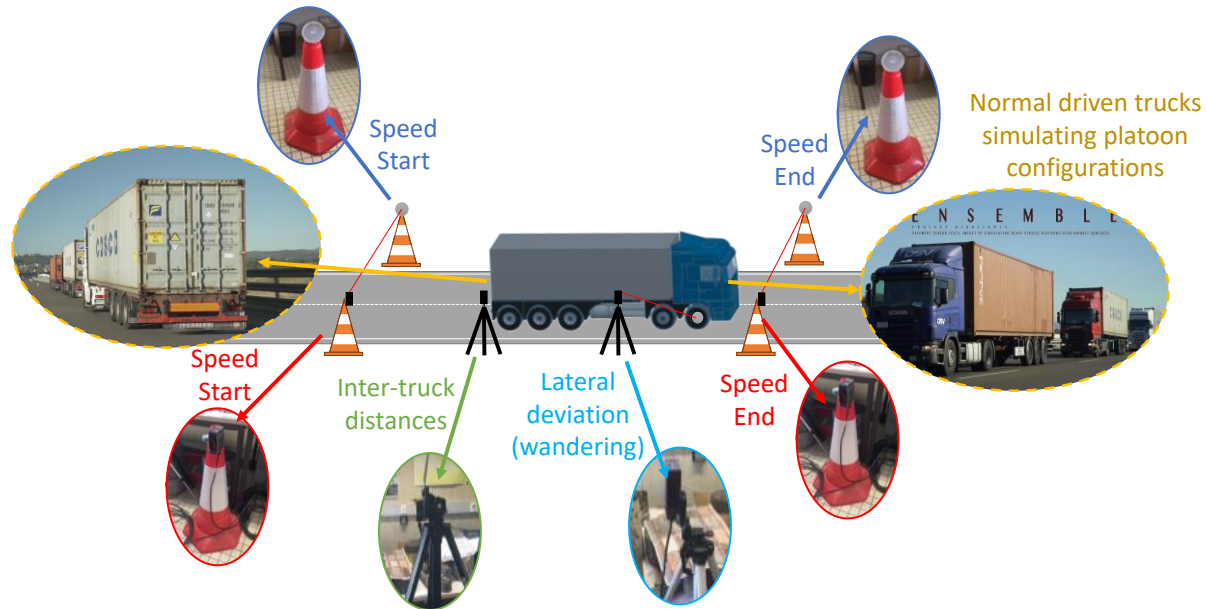


(a) Truck loads



(b) lateral deviation (wandering)

16 **FIGURE 3 Truck-loads, lateral deviation (wandering) and laser system.**



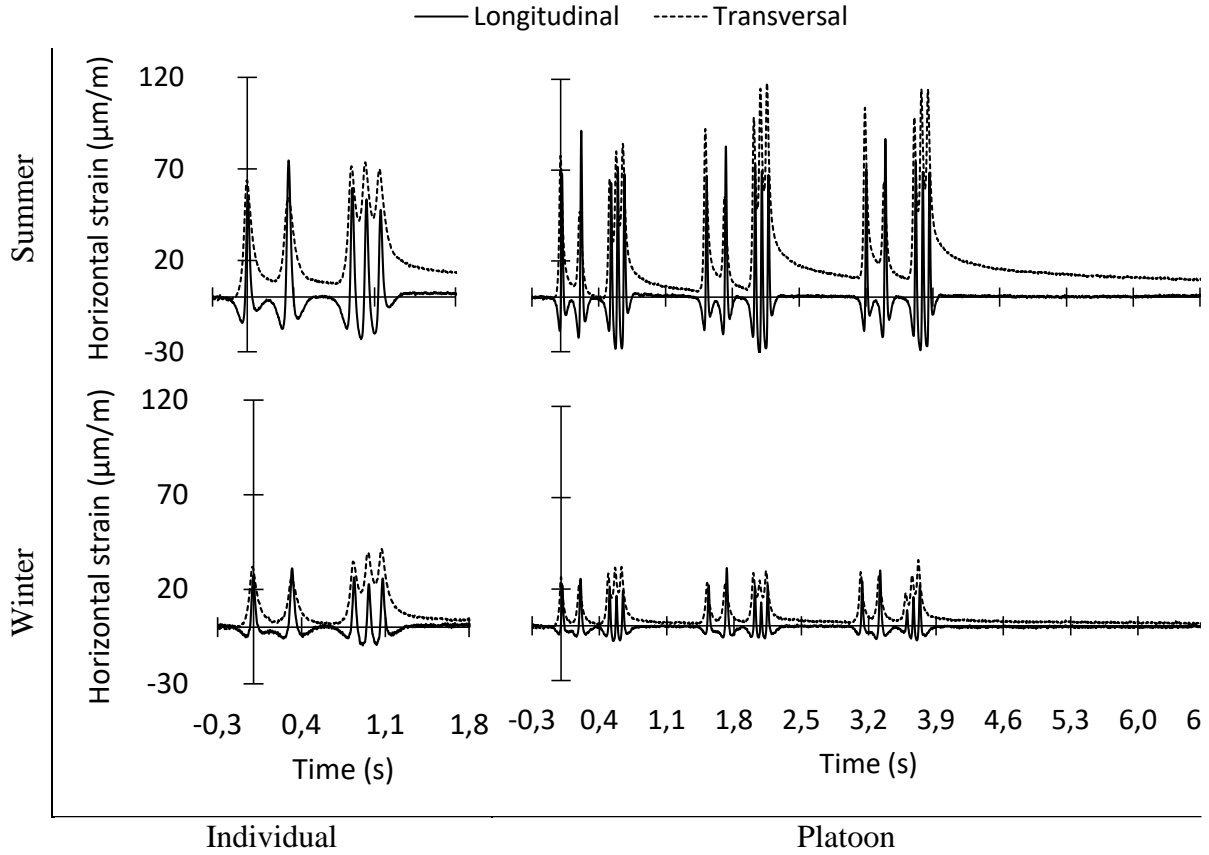
1
2 **FIGURE 4 Laser system for monitoring truck speeds, and longitudinal and lateral positions**

3. EXAMPLES OF MEASURED STRAIN SIGNALS

3
4
5 Figure 5 presents examples of longitudinal and transversal strain signals measured at the bottom of
6 the base course, at 25cm depth from the pavement surface, during the winter and summer test
7 campaigns. The figure compares signals obtained for an individual truck, and the platoon of 3
8 trucks, at a speed of 40km/h. The selected signals correspond to truck passages where the lateral
9 wandering is close to 0, which means that the truck wheels are centered on the position of the strain
10 gauges. For this position, the tensile strains recorded by the gages are maximum. The following
11 observations can be made on these strain signals:

- 12 • Strains measured in summer (at temperatures between 25.0°C and 27.5°C) are much higher
13 than the strains measured in the winter (at temperatures between 6.1°C and 11.3°C)
- 14 • The shape of the longitudinal and transversal strain signals is very different. The
15 longitudinal signals present alternatively strains in compression (negative) and in extension
16 (positive). The transversal strains are only in extension.
- 17 • The tensile strain values are significantly higher in the transversal direction due to the single
18 wheels of the trailer tridem axles of the semitrailer trucks commonly used in Europe at
19 present [31]. This could explain the predominant emergence of longitudinal cracking
20 patterns on the pavement surface.
- 21 • The transversal strain signals present delayed deformations that are only slowly recovered
22 after the passage of the vehicles due to the viscoelastic behavior of asphalt materials. These
23 delayed deformations increase with temperature (summer conditions) and when inter-
24 vehicle distance is small (platoon configuration).

25
26 Considering that the main objective of this work is the study of the fatigue cracking phenomena
27 under individual and platoon truck configurations, in the next part of the paper, the analysis will
28 focus only on the transversal strain signals, which generate the highest tensile strains, with values
29 slowly returning to zero and possibly some permanent deformations.
30



1
2 **FIGURE 5** Examples of longitudinal and transversal strain signals obtained at 25 cm depth
3 from the pavement surface (at the bottom of the base course) for a test speed of 40 km/h.

4 **4. DATA TREATMENT – CALCULATION OF PAVEMENT DAMAGE**

5
6 **4.1 Definition of fatigue damage and calculation of the Coefficient of Aggressiveness**

7
8 The concept of Coefficient of Aggressiveness (CA) of a vehicle, used in the French pavement
9 design method, is introduced to evaluate and compare the fatigue damage produced by the different
10 vehicle configurations.

11
12 In the case of fatigue damage, the Coefficient of Aggressiveness of a vehicle is defined as the α -
13 factor (in percentage) of the ratio between the fatigue damage produced by a given truck and the
14 damage produced by the equivalent standard axle (ESAL), which is a single axle with dual wheels,
15 loaded at 130 kN in the French pavement design method. The value of the α -factor corresponds to
16 the accepted level of damage corresponding to the end of service life of the pavement (20% in this
17 paper case study). According to this definition, the CA of a truck can be defined by Equation 3.

18

$$CA_{truck} = \alpha * \frac{d_{truck}}{d_{ESAL}} = \alpha \sum_{i=1}^n \left(\frac{d_{Axle_i}}{d_{ESAL}} \right) \quad (3)$$

1 Where, d_{truck} is the fatigue damage produced by the whole truck, d_{ESAL} is the fatigue damage
 2 produced by the equivalent standard axle (130 kN axle), d_{Axle_i} is the damage produced by the i^{th}
 3 axle of the truck and n is the number of axles of the truck.

4
 5 The concept of cumulative damage is used for the calculation of the fatigue damage d produced by
 6 a single load. With this approach, the elementary damage produced by one load can be simply
 7 defined by Equation 4.

$$d = \frac{1}{N_f} \quad (4)$$

9
 10 Where, N_f is the number of load cycles leading to failure, defined using the fatigue model.

11
 12 In this study, in order to consider complex strain signals, the number of cycles to failure N_f due to
 13 each truck axle (steer axle, driven axle, and trailer tridem) was calculated using the fatigue model
 14 for multiple axle loads proposed by Homsy (Equation 2). This equation is based on the shape
 15 parameters of the strain signals registered from the passage of isolated single, tandem and tridem
 16 axles in the Accelerated Pavement Testing (APT) facilities of Gustave Eiffel University.

17
 18 In the case of the strain signal corresponding to the reference 130 KN axle, as this signal was not
 19 measured, it was obtained by modeling, using the multilayered elastic software ALIZE, for the
 20 same pavement structure, same temperature, and loading speed conditions.

21
 22 From all the experimental data, only four-strain signals where the lateral wandering values between
 23 passages for the individual trucks and platoon configuration was less than 20 cm for both test
 24 campaigns were considered. In the case of the summer campaign, four additional strain signals
 25 with an increased lateral wandering (40 cm) were added to compare the effect of this increased
 26 lateral wandering.

27
 28 Finally, to evaluate the fatigue life and fatigue damage corresponding to different traffic scenarios,
 29 the approach of the French pavement design method was followed. In this approach, after
 30 determining the Coefficient of Aggressiveness of each truck (CA_{truck}), according to equation 4, a
 31 mean coefficient of aggressiveness corresponding to the total cumulative traffic called CAM is
 32 determined according to Equation 5.






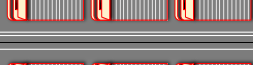




$$CAM = \frac{1}{N_{truck}} \sum_{j=i}^{N_{truck}} CA_{truck_j} \quad (5)$$

34
 35 Where, N_{truck} is the total number of trucks considered, and CA_{truck_j} the coefficient of
 36 aggressiveness of truck j . With this definition, the CAM value can also be defined as the coefficient
 37 which is used to convert the number of trucks in a traffic N_{truck} into the corresponding number of
 38 ESALs, designated by NE Equation 6).

$$NE = CAM \times N_{truck} \quad (6)$$

4.2 Traffic scenarios for the calculation of pavement fatigue life.

- 1 To evaluate the impact of different proportions of platoons in the heavy vehicle traffic, five
 2 different traffic scenarios (shown in Figure 6) have been considered:
- 3 • The reference scenario represents traffic with no platoons and with a lateral wandering of
 4 the vehicles of 20 cm
 - 5 • Scenario 1 represents traffic with 100% of platoons in the winter and no platoons in the
 6 summer, with the same lateral wandering of 20 cm.
 - 7 • Scenario 2 represents traffic with 100% of platoons in the summer and no platoons in the
 8 winter, with the same lateral wandering of 20 cm.
 - 9 • Scenario 3 represents traffic with 100% of platoons during the whole year, with the same
 10 lateral wandering of 20 cm.
 - 11 • Scenario 4 represents traffic with 100% of platoons during the whole year, but with an
 12 increased lateral wandering of 40 cm
 13

Reference	Campaign: Winter, Wandering = 20 cm, Conf: Individual (0% platoon penetration) $ADT = ADT_{Jan}$	
	Campaign: Summer, Wandering = 20 cm, Conf: Individual (0% platoon penetration) $ADT = ADT_{Aug}$	
Scenario 1	Campaign: Winter, Wandering = 20 cm, Conf: Platoon (100% platoon penetration) $ADT = ADT_{Jan}$	
	Campaign: Summer, Wandering = 20 cm, Conf: Individual (0% platoon penetration) $ADT = ADT_{Aug}$	
Scenario 2	Campaign: Winter, Wandering = 20 cm, Conf: Individual (0% platoon penetration) $ADT = ADT_{Jan}$	
	Campaign: Summer, Wandering = 20 cm, Conf: Platoon (100% platoon penetration) $ADT = ADT_{Aug}$	
Scenario 3	Campaign: Winter, Wandering = 20 cm, Conf: Platoon (100% platoon penetration) $ADT = ADT_{Jan}$	
	Campaign: Summer, Wandering = 20 cm, Conf: Platoon (100% platoon penetration) $ADT = ADT_{Aug}$	
Scenario 4	Campaign: Winter, Wandering = 40 cm, Conf: Platoon (100% platoon penetration) $ADT = ADT_{Jan}$	
	Campaign: Summer, Wandering = 40 cm, Conf: Platoon (100% platoon penetration) $ADT = ADT_{Aug}$	

14
 15 **FIGURE 6 Scenarios of analysis.**

16
 17
 18
 19
 20
 21

1 These traffic scenarios have been applied to calculate the fatigue life of the pavement structure of
2 the full-scale experiment (Figure 2). For these fatigue life calculations, typical data corresponding
3 to heavy traffic roads, category T00 according to EU definitions were used:

- 4 - An Average Daily truck traffic (ADT, for the weighing highways in Spain where the
5 experiment took place) of 15951 for winter and 28587 for summer was used, corresponding
6 to a two-way road with light and heavy vehicles, according to the traffic database of the
7 Spanish Road and Highway Administration [32].
- 8 - The corresponding cumulative traffic was then calculated using Equation 7.

$$N = T * C * L * D * 365 * ADT \quad (7)$$

10 With, T : Percentage of trucks in the ADT, January: 18% and August: 13% [32]. C : Annual traffic
11 growth factor (Equation 4, for g : annual traffic growth rate, January: 3,3% and August: 3,1% [32]).
12 D and L : Direction Distribution Factor and Lane Distribution Factor, which were considered 50%
13 and 85% for a two-way road with three lanes by traffic direction, according the Spanish Order
14 FOM/3460/2003 [33].

$$C = \frac{(1 + g)^p - 1}{g} \text{ for } g \neq 0 \quad (8)$$

16 **5. PAVEMENT DAMAGE AND PAVEMENT FATIGUE LIFE RESULTS**

18 **5.1. Winter tests campaign**

19 As described before, the equation proposed by Homsí [25]–[27], [30] for multiple axle
20 configurations was used to determine the number of cycles to fatigue for each truck under each
21 load configuration and test campaign. The different parameters of the fatigue model obtained for
22 each axle (Axle 1: single wheels, Axle 2: dual wheels, and Axle 3: tridem with single tires), for
23 each truck, either in single truck configuration or in platoon configuration, are shown in Figure 7.

24 For this winter test campaign, there is no significant difference between the model parameters
25 obtained for the single trucks and the platoon, probably because for the temperature range
26 corresponding to this campaign (between about 6 and 11 °C), the behavior of the pavement is
27 relatively elastic, and there is no significant effect due to the application of multiple truck loads in
28 a short time interval.

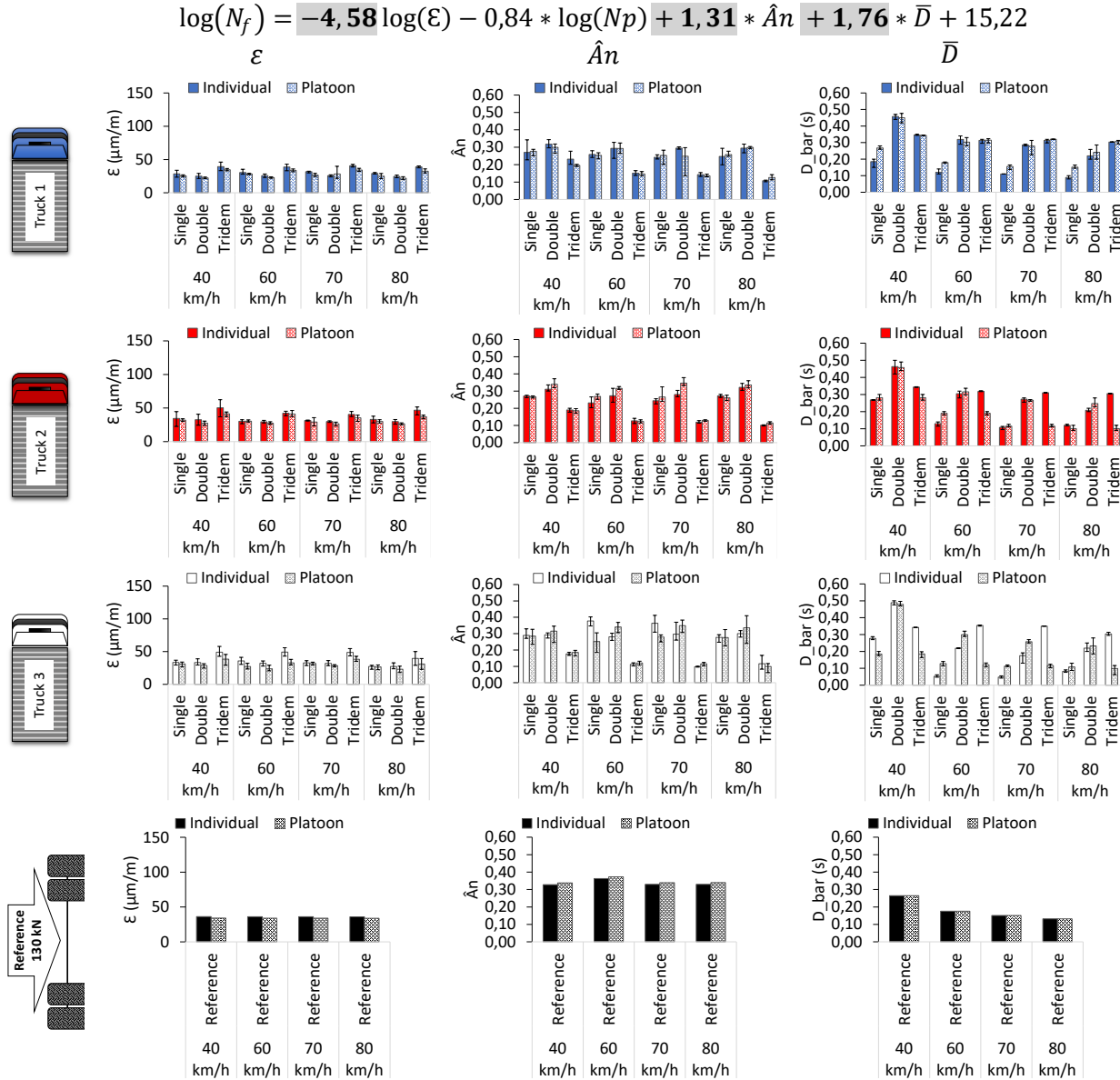
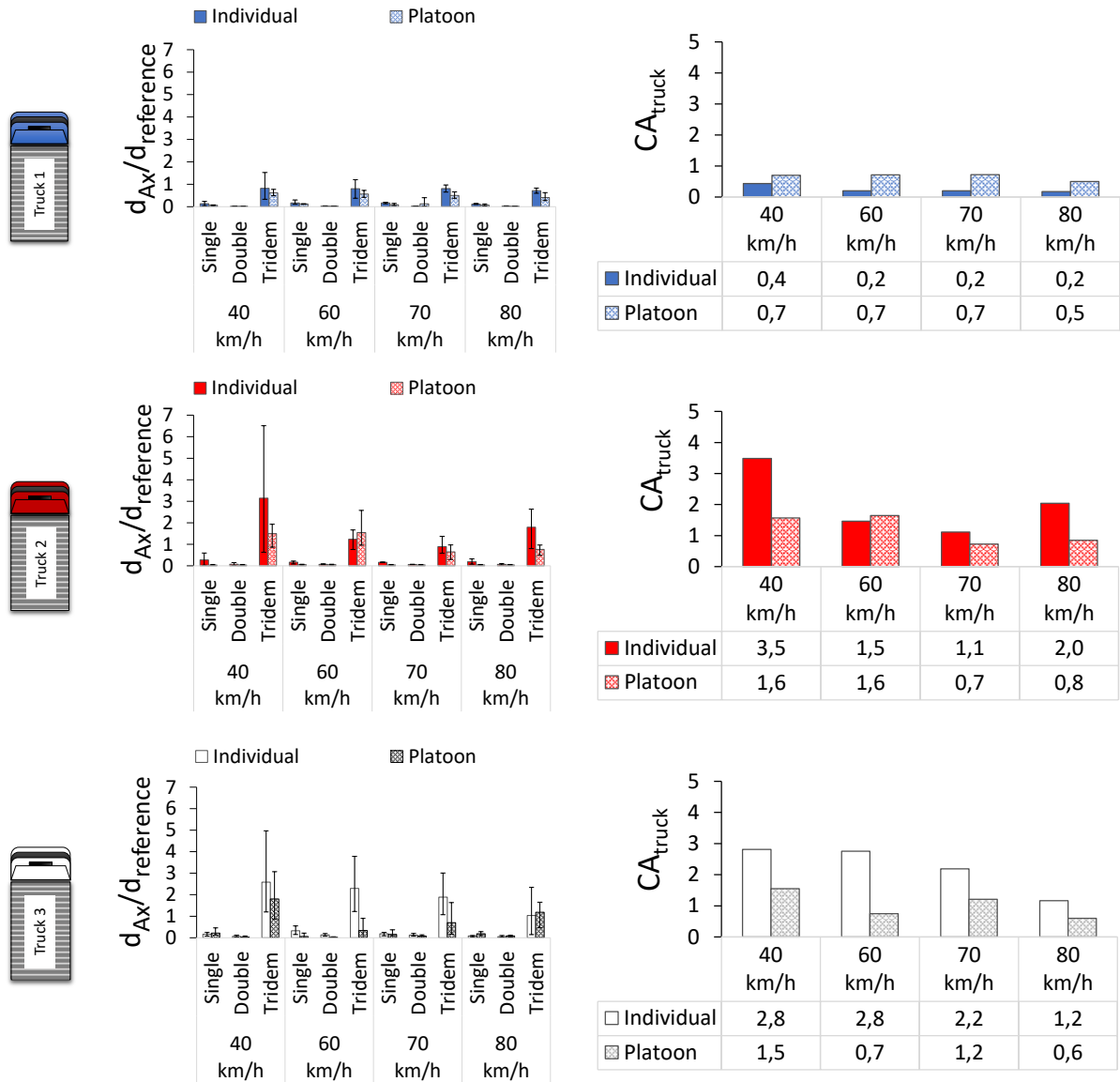


FIGURE 7 Fatigue parameters of the strain signals for the winter campaign (tension is considered positive). Fatigue coefficients obtained from [25]–[27], [30]. **Single:** steer axle, **Double:** driven axle and **Tridem:** trailer tridem axle.

The relationship between the damage obtained from each axle and the equivalent standard axle (130 kN) (which represents the aggressiveness of each individual axle) is shown in Figure 8. This figure shows that the tridem axles cause the highest damage, as was expected. The corresponding coefficients of aggressiveness for entire trucks (CA_{truck} , Equation 3), calculated for a level of damage of 20% of the pavement, are also shown in the same figure. The results indicate that:

- The CA_{truck} values are a little higher for truck 2 and truck 3 (for the individual trucks), which can be due to probably the natural variability of the test (temperature, position of the wheels, differences in axle loads).

- There is no clear difference between the CA_{truck} values obtained for the individual trucks and for the platoons. In some cases, for trucks 2 and 3, the individual trucks are more aggressive than in the platoon. This means that for cold temperatures (here around 10°C), platooning does not seem to create more fatigue damage than individual trucks (for the configurations considered in this experiment).

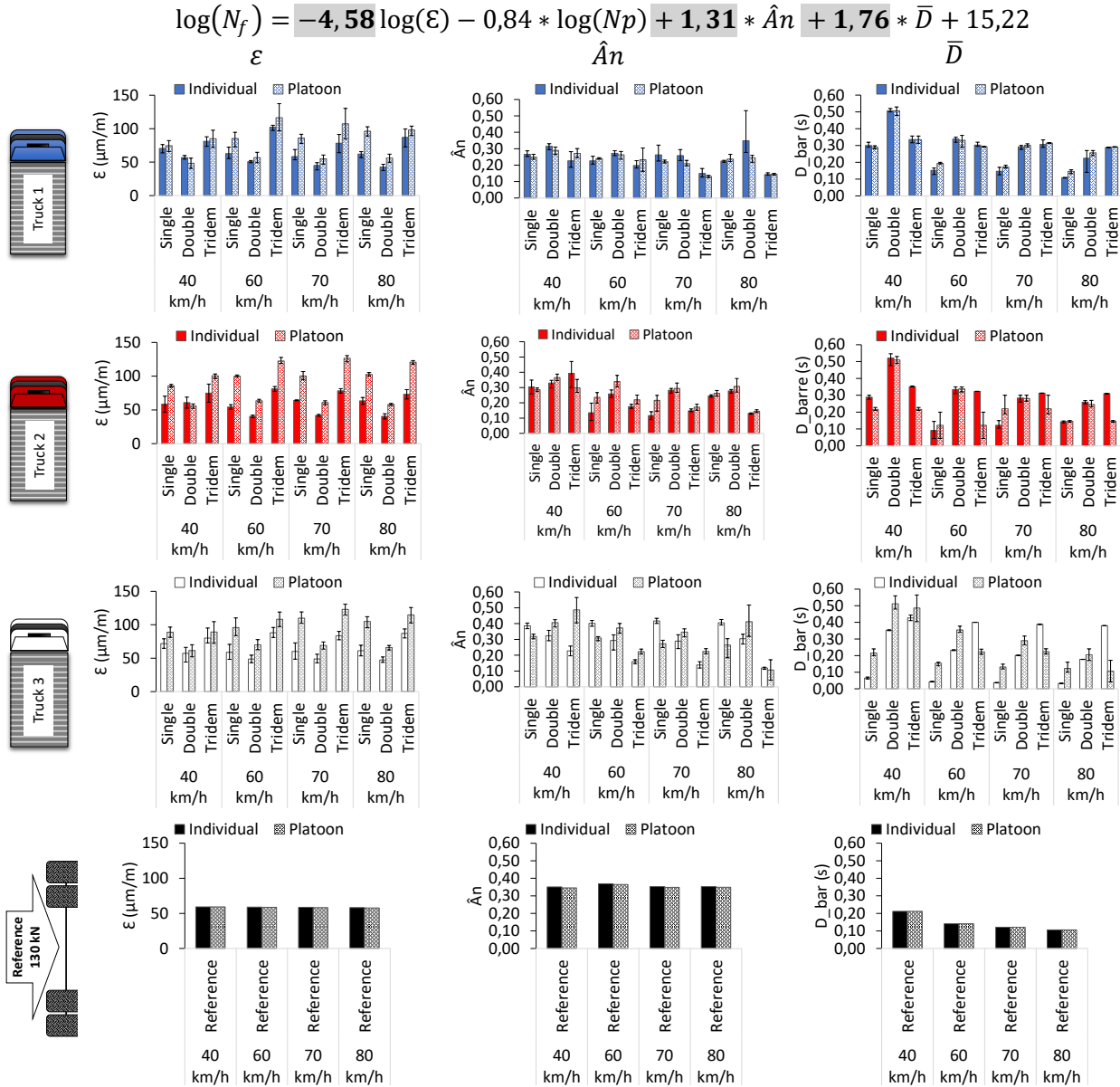


7
8 **FIGURE 8** Values of fatigue damage induced by each truck axle (relatively to the reference
9 **130 kN axle**), and CA_{truck} values of the different trucks, for the winter test campaign.

10 **5.2. Summer campaign**

11
12 Figure 9 shows, for the summer campaign, the values of the parameters of the fatigue model of
13 Homsy, for each truck and each axle, under both individual and platoon load configurations.
14 Understanding that the positive or negative sign of each coefficient in the multi-axle fatigue
15 equation indicates an increase or decrease in the number of cycles to fatigue, the results indicate

1 that: (1) platoons increase the maximum transversal strain values and (2) platoons also decrease in
 2 general the positive normalized area under the transversal strain signal. As a result, the platoon
 3 configuration reduces the number of cycles to fatigue, for the test conditions present in summer
 4 (temperatures between about 25 °C and 27 °C).
 5

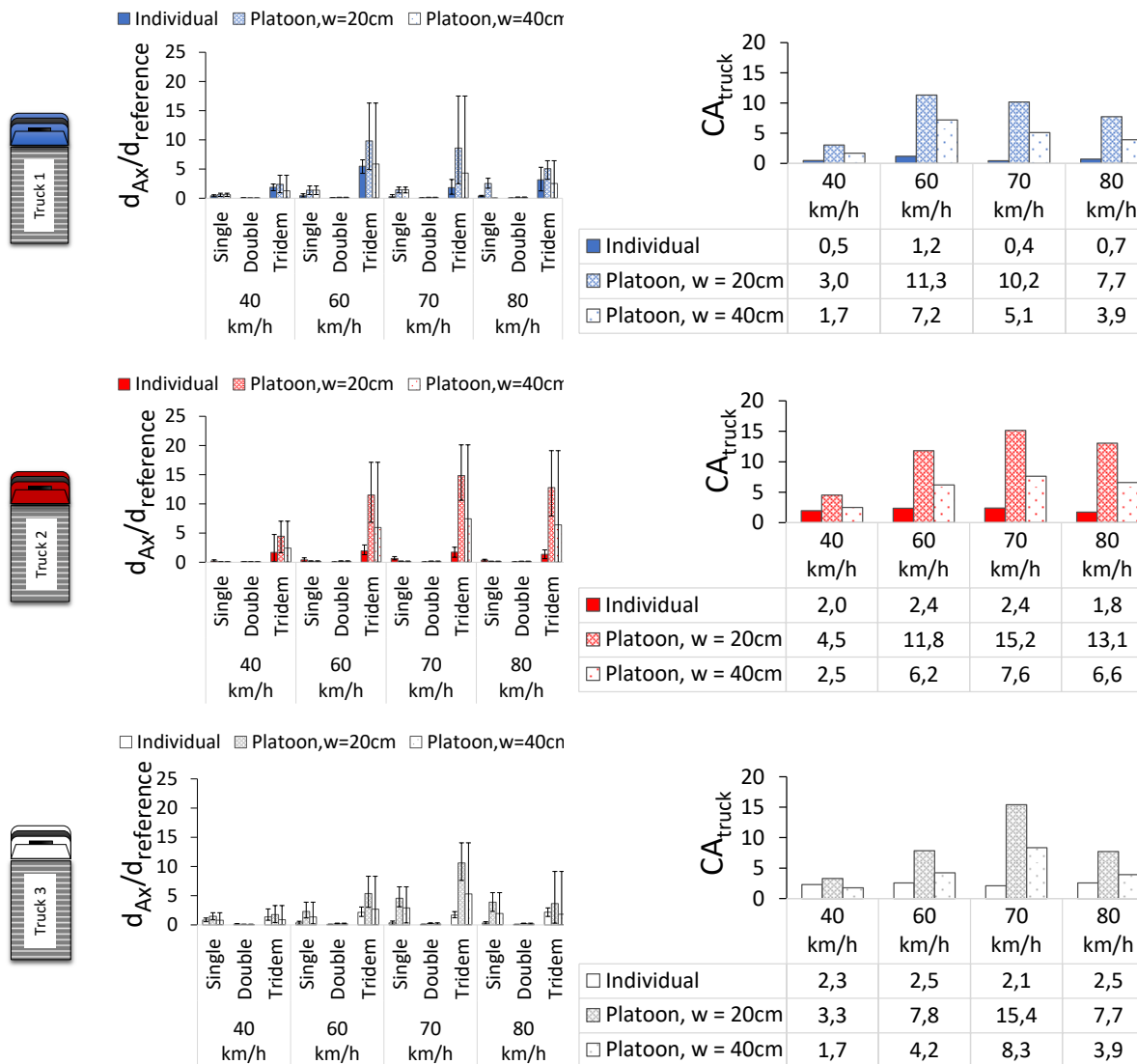


6
 7 **FIGURE 9** Fatigue parameters of the strain signals for the summer campaign (tension is
 8 considered positive). Fatigue coefficients obtained from [25]–[27], [30]. Single: steer axle,
 9 Double: driven axle and Tridem: trailer tridem axle.

10 Figure 10 shows the damage ratios of each axle, relatively to the reference 130 kN axle. The highest
 11 damage values are obtained for the tridem axles, in the platoon truck configuration. The
 12 aggressiveness values of each truck, CA_{truck} are also shown in this figure. It can be seen that:

- In the individual truck configuration, the CA_{truck} values are very similar for all the test speeds, with some variations between trucks, due to the variation in the loads and inter-axle distances between trucks.
- In the platoon configuration, contrary to what was observed in the winter campaign, the CA_{truck} values significantly increase for the three trucks of the platoon, and vary with truck speed. Again, this can be attributed to a more viscoelastic behavior of the asphalt layers at these higher temperatures.
- Additionally, increasing the lateral wander significantly reduces the aggressiveness (CA_{truck} values) of the platoons.

In conclusion, for the warm summer temperatures (here about 27 °C), platooning clearly increases fatigue damage compared with individual trucks. The values are between 28% and 376% higher for a wandering equal to 20 cm at all the test speeds.



15
16 **FIGURE 10** Values of fatigue damage per axle and CA_{truck} values for the summer campaign.

3.4. Fatigue life for the different traffic scenarios

Using the CA_{truck} values displayed in the previous sections, it is possible to predict the corresponding number of ESALs by each half-year for the pavement test section under study. The accumulation of this value compared to the number of cycles to fatigue projected by the use of the Homsy fatigue equation, represents the fatigue damage for the structure. In this sense, considering reaching 20% of fatigue damage for each traffic scenario, Figure 11 shows the corresponding remaining fatigue lives expressed in years. In comparison to the reference scenario, which represents the passage of fully loaded 5-axle semi-trailers, in individual configurations, the following trends are observed:

- The first scenario, corresponding to a traffic distribution with 100% of platoons during the winter and no platoons during the summer, does not change the remaining fatigue life of the pavement structure.
- On the contrary, scenarios 2 and 3, corresponding to a traffic distribution with 100% of platoons just during summer or all along the year, significantly decrease the remaining fatigue life, with a maximum reduction of -68% at 70 km/h.
- However, as shown in scenario 4, this effect can be reduced by increasing the lateral wander of the platoons, which is also supported by other results from the literature [4], [17], [18], [20]–[22], [24].

Considering that these measurements were done with fully loaded trucks, and assuming 100% platoon penetration, the negative impact of platoons could be reduced by varying these parameters, as well as by changing the inter-truck distances [17] the truck speeds, and also the time of the day [23] at which platoons are allowed to circulate. It is important to add that the CA values determined in this study are only valid for this pavement structure. Therefore, for different conditions, the corresponding values should be appropriately calibrated.

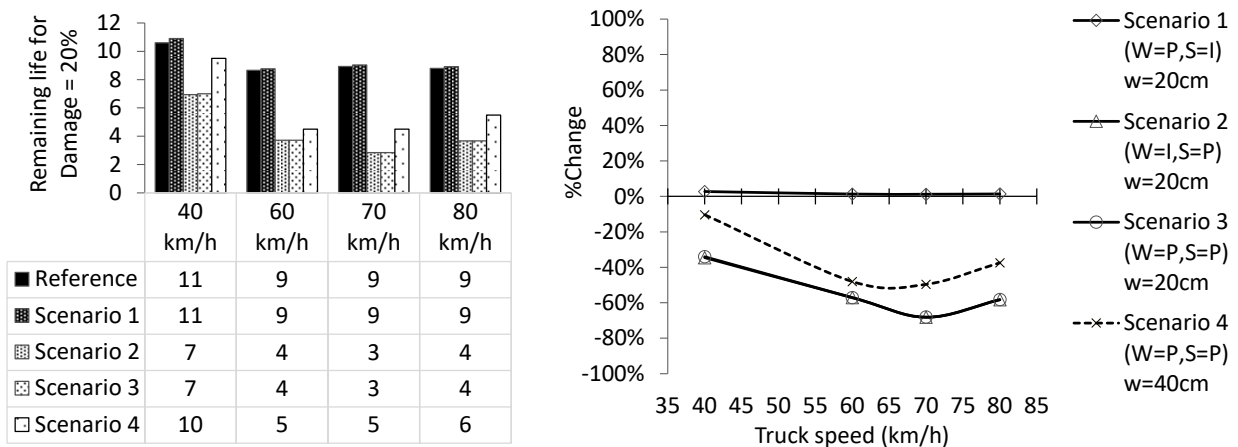


FIGURE 11 Calculated pavement fatigue lives, for 20% of damage, for different platoon traffic scenarios.

3. CONCLUSIONS

This paper presents the results of a study on the effect of platoons on the fatigue life predictions of a European pavement test section. The test protocol and the data treatment proposed in this document are based on an original fatigue model for multiple axle loads, which considers the maximum tensile strain, the number of peaks of the strain signal, the area, and the duration of the strain signal. This approach was applied to strain signals measured by strain gauges installed in an experimental pavement section but can also be used with strain signals obtained by modeling. The following conclusions can be drawn from this study:

- The strain measurements performed on the pavement structure, under 5-axle semi-trailer truck loading, indicated that at the bottom of the asphalt layers, the transversal strains were significantly higher than the longitudinal strains. Strain accumulation effects were also more important for transversal strains, especially at high temperatures (during the summer test campaign).
- With the fatigue model used, which considers the shape of the strain signals, it was clearly shown that for the same loading conditions (same axle loads, speed, and lateral wander), the fatigue damage produced by platoons (compared with single trucks) varies significantly with temperature. At low temperatures (around 10 °C), there was no difference between the damage induced by individual trucks and by platoons. However, at higher temperatures (around 27°C), the damage induced by platoons was significantly higher due to strain accumulation under multiple loads.
- Despite the good predictions obtained with the new fatigue model, further research is carried out, based on laboratory studies, to consider better the most significant effects related to platoon loadings: influence of rest periods and accumulated deformations.
- For the case study presented in this document, truck platoon configurations showed considerably higher fatigue life reductions during summer. In this sense, limiting platooning along this season, or potentially during hours with the highest temperatures, could be a possible management strategy to limit/avoid early pavement fatigue damage. It was also found that the lateral wandering of the trucks has a significant effect and that increasing the lateral wandering could also help limit fatigue damage.
- Following these results, the ENSEMBLE work package related to infrastructure is currently developing further research studies based on parametric studies with a pavement modeling program. The objective is to make a more general analysis of the effects: (1) traffic distribution along the year and along the time of the day, (2) percentage of platoon penetration in the daily and annual traffic, (3) level of loading of the trucks, number of trucks in platoon configuration, (4) lateral wandering, (5) inter-truck distances and (6) representative existing pavement structures. From these simulations, recommendations to limit the impact of platoons will be proposed.

AUTHOR CONTRIBUTIONS

The authors confirm contribution to the paper as follows: study conception and design: P. Leiva-Padilla, J. Blanc, F. Hammoum, P. Hornych; data collection: J. Blanc, A. Salgado; analysis and interpretation of results: P. Leiva-Padilla, J. Blanc, F. Hammoum, P. Hornych; draft manuscript preparation: P. Leiva-Padilla. All authors reviewed the results and approved the final version of the manuscript.

1 **ACKNOWLEDGES**

2
3 The research presented in this paper is part of the European project ENSEMBLE, which is co-
4 funded by the EU under the Horizon2020 Research and Innovation Program, grant agreement No
5 769115.

6 **REFERENCES**

- 7
8 [1] H. Noorvand, G. Karnati, and B. S. Underwood, "Autonomous vehicles: Assessment of the
9 implications of truck positioning on flexible pavement performance and design," *Transp.*
10 *Res. Rec.*, 2017, doi: 10.3141/2640-03.
11 [2] A. Ladino, L. Xiao, K. Adjenugwhure, N. Deschle, and G. Klunder, "Cross-Platform
12 Simulation Architecture with application to truck platooning impact assessment," 2021.
13 [3] E. Mascalchi, A. Coda, and D. Willemsen, "Specifications for multi-brand truck platooning,"
14 2020.
15 [4] O. E. Gungor, R. She, I. L. Al-Qadi, and Y. Ouyang, "One for all: Decentralized optimization
16 of lateral position of autonomous trucks in a platoon to improve roadway infrastructure
17 sustainability," *Transp. Res. Part C Emerg. Technol.*, 2020, doi: 10.1016/j.trc.2020.102783.
18 [5] Y. Suzuki, "A new truck-routing approach for reducing fuel consumption and pollutants
19 emission," *Transp. Res. Part D Transp. Environ.*, 2011, doi: 10.1016/j.trd.2010.08.003.
20 [6] T. Robinson, E. Chan, and E. Coelingh, "Operating platoons on public motorways: An
21 introduction to the SARTRE platooning programme," 2010.
22 [7] M. M. Hoque, Q. Lu, A. Ghiasi, and C. Xin, "Highway Cost Analysis for Platooning of
23 Connected and Autonomous Trucks," *J. Transp. Eng. Part A Syst.*, vol. 147, no. 1, 2021,
24 doi: 10.1061/JTEPBS.0000474.
25 [8] L. Konstantinopoulou, A. Coda, and F. Schmidt, "Specifications for Multi-Brand Truck
26 Platooning," in *ICWIM 8, 8th International Conference on Weigh-In-Motion, May 2019*,
27 2019, p. 8.
28 [9] J. Thunberg, N. Lyamin, K. Sjoberg, and A. Vinel, "Vehicle-to-Vehicle Communications for
29 Platooning: Safety Analysis," *IEEE Netw. Lett.*, vol. 1, no. 4, 2019, doi:
30 10.1109/lnet.2019.2929026.
31 [10] A. Alam, B. Besselink, V. Turri, J. Martensson, and K. H. Johansson, "Heavy-duty vehicle
32 platooning for sustainable freight transportation: A cooperative method to enhance safety
33 and efficiency," *IEEE Control Syst.*, 2015, doi: 10.1109/MCS.2015.2471046.
34 [11] C. Bonnet and H. Fritz, "Fuel consumption reduction in a platoon: Experimental results with
35 two electronically coupled trucks at close spacing," 2000, doi: 10.4271/2000-01-3056.
36 [12] S. Tsugawa, S. Jeschke, and S. E. Shladovers, "A review of truck platooning projects for
37 energy savings," *IEEE Trans. Intell. Veh.*, 2016, doi: 10.1109/TIV.2016.2577499.
38 [13] S. Tsugawa, "Results and issues of an automated truck platoon within the energy ITS
39 project," 2014, doi: 10.1109/IVS.2014.6856400.
40 [14] S. Eilers *et al.*, "COMPANION-Towards Co-operative Platoon Management of Heavy-Duty
41 Vehicles," 2015, doi: 10.1109/ITSC.2015.208.
42 [15] M. P. Lammert, A. Duran, J. Diez, K. Burton, and A. Nicholson, "Effect of Platooning on
43 Fuel Consumption of Class 8 Vehicles Over a Range of Speeds, Following Distances, and
44 Mass," *SAE Int. J. Commer. Veh.*, 2014, doi: 10.4271/2014-01-2438.
45 [16] H. L. Humphreys, J. Batterson, D. Bevly, and R. Schubert, "An Evaluation of the Fuel
46 Economy Benefits of a Driver Assistive Truck Platooning Prototype Using Simulation,"
47 2016, doi: 10.4271/2016-01-0167.
48 [17] O. E. Gungor and I. L. Al-Qadi, "All for one: Centralized optimization of truck platoons to
49 improve roadway infrastructure sustainability," *Transp. Res. Part C Emerg. Technol.*, 2020,

- 1 doi: 10.1016/j.trc.2020.02.002.
- 2 [18] F. Chen, M. Song, X. Ma, and X. Zhu, "Assess the impacts of different autonomous trucks'
- 3 lateral control modes on asphalt pavement performance," *Transp. Res. Part C Emerg.*
- 4 *Technol.*, 2019, doi: 10.1016/j.trc.2019.04.001.
- 5 [19] F. Chen, M. Song, and X. Ma, "A lateral control scheme of autonomous vehicles considering
- 6 pavement sustainability," *J. Clean. Prod.*, 2020, doi: 10.1016/j.jclepro.2020.120669.
- 7 [20] M. Song, F. Chen, and X. Ma, "Organization of autonomous truck platoon considering
- 8 energy saving and pavement fatigue," *Transp. Res. Part D Transp. Environ.*, vol. 90, 2021,
- 9 doi: 10.1016/j.trd.2020.102667.
- 10 [21] F. Zhou *et al.*, "Optimization of Lateral Wandering of Automated Vehicles to Reduce
- 11 Hydroplaning Potential and to Improve Pavement Life," *Transp. Res. Rec.*, 2019, doi:
- 12 10.1177/0361198119853560.
- 13 [22] O. E. Gungor and I. L. Al-Qadi, "Wander 2D: a flexible pavement design framework for
- 14 autonomous and connected trucks," *Int. J. Pavement Eng.*, 2020, doi:
- 15 10.1080/10298436.2020.1735636.
- 16 [23] M. M. Rana and K. Hossain, "Simulation of autonomous truck for minimizing asphalt
- 17 pavement distresses," *Road Mater. Pavement Des.*, 2021, doi:
- 18 10.1080/14680629.2021.1883469.
- 19 [24] P. Marsac *et al.*, *Optimization of truck platoon wander patterns based on thermo-*
- 20 *viscoelastic simulations to mitigate the damage effects on road structures*, vol. 96 LNCE.
- 21 2020.
- 22 [25] F. Homsy, D. Bodin, S. Yotte, D. Breyse, and J. M. Balay, "Multiple axle loadings: Shape
- 23 parameters and their effect on the fatigue life of asphalt mixtures," *Eur. J. Environ. Civ.*
- 24 *Eng.*, 2010, doi: 10.3166/EJECE.15.743-758.
- 25 [26] F. Homsy, D. Bodin, S. Yotte, D. Breyse, and J. M. Balay, "Fatigue life modelling of asphalt
- 26 pavements under multiple-axle loadings," *Road Mater. Pavement Des.*, 2012, doi:
- 27 10.1080/14680629.2012.711924.
- 28 [27] F. Homsy, D. Bodin, D. Breyse, S. Yotte, and J. M. Balay, "A multi-linear fatigue life model
- 29 of flexible pavements under multiple axle loadings," *RILEM Bookseries*, 2012, doi:
- 30 10.1007/978-94-007-4566-7_68.
- 31 [28] M. A. Miner, "Cumulative Damage in Fatigue," *J. Appl. Mech.*, vol. 12, pp. A159–A164,
- 32 1945.
- 33 [29] European Committee for Standardization, "EN 12697-24: 2018, Bituminous mixtures. Test
- 34 methods. Part 24: Resistance to fatigue." .
- 35 [30] F. Homsy, J. M. Balay, D. Bodin, D. Breyse, and S. Yotte, "Estimating truck aggressiveness
- 36 using a multilinear fatigue model and a viscoelastic pavement model," *J. Transp. Eng.*,
- 37 2016, doi: 10.1061/(ASCE)TE.1943-5436.0000811.
- 38 [31] European Commission Directorate General Transport, "Cost 334 Effects of Wide Single
- 39 Tyres and Dual Tyres. Final Report of the Action," 2001.
- 40 [32] Dirección General de Carreteras, "Gobierno de España - Ministerio de Transportes,
- 41 Movilidad y Agenda Urbana." https://www.mitma.es/carreteras#Red_de_carreteras
- 42 (accessed Jun. 04, 2021).
- 43 [33] E. M. de Fomento, "Instrucción de carreteras. Norma 6.1 IC: Secciones de firme," *Norm.*
- 44 *Instr. Construcción*, 2003.
- 45